

Background Document

FEMA P-58/BD-3.9.7

Fragility of Masonry Chimneys

Prepared by

John Oстераas, Exponent, Menlo Park, California
Helmut Krawinkler, Stanford University, Stanford, California

Submitted to

APPLIED TECHNOLOGY COUNCIL
201 Redwood Shores Parkway, Suite 240
Redwood City, California 94065
www.ATCouncil.org

Prepared for

FEDERAL EMERGENCY MANAGEMENT AGENCY
U.S. Department of Homeland Security
500 C Street, SW
Washington, D.C. 20472

December 8, 2010



FEMA



Background Documentation

FEMA P-58 Background Documents are a series of reports documenting the technical background and source information for key aspects of the FEMA P-58 methodology and its implementation. These reports were developed over the course of the 10-year ATC-58/ATC-58-1 Projects funded under FEMA Contracts EMW-2001-RP-0056 and HSFEHQ-06-D-1105.

Background Documents were developed by consultants, serving at various levels within the project hierarchy, reporting the results of: (1) decisions on technical development protocols; (2) focused studies on the development of key aspects of the methodology; (3) documentation of recommended procedures; and (4) collection of available data for the development of structural and nonstructural fragilities. They were initially intended to serve as a record of the technical state-of-knowledge at the time they were produced, and as resources for the development of the eventual project reports. As such, they represent a snapshot in time, and may, or may not, match the technical content, recommended procedures, or data incorporated into the final methodology and its implementation.

This Background Document is intended for the purpose of providing supplemental knowledge to users of the FEMA P-58 methodology. Information contained herein has not been independently verified for accuracy as a stand-alone document, and may have been superseded in its final implementation within the methodology. Specifically in the case of certain nonstructural component fragilities, the NISTIR fragility classification numbering scheme was modified over the course of the project, and the fragility classification number assigned in this document might be different from numbers assigned in the final fragility database. Users of information in this document assume all liability arising from such use.

Notice

Any opinions, findings, conclusions, or recommendations expressed in this publication do not necessarily reflect the views of the Applied Technology Council (ATC), the Department of Homeland Security (DHS), or the Federal Emergency Management Agency (FEMA). Additionally, neither ATC, DHS, FEMA, nor any of their employees, makes any warranty, expressed or implied, nor assumes any legal liability or responsibility for the accuracy, completeness, or usefulness of any information, product, or process included in this publication. Users of information from this publication assume all liability arising from such use.

Cover illustration – Primary resource documents for the FEMA P-58 *Seismic Performance Assessment of Buildings, Methodology and Implementation* series of products: FEMA P-58-1, *Volume 1 – Methodology*, and FEMA P-58-2, *Volume 2 – Implementation Guide*.

Fragility of Masonry Chimneys

John Osteraas and Helmut Krawinkler (12/08/2010)

Table 1. Summary results



Fragility, damage measures, and consequences for:		
Component category:	Masonry chimneys, excluding industrial chimneys	
Basic composition:	Unreinforced masonry chimney as a component of woodframe building, including firebox and chimney, excluding interior veneer and ornamentation. May also include chimneys where presence of quality of reinforcing is unknown.	
Units:	Single chimney	
Demand parameter:	Peak horizontal ground accelerations	
Number of damage states:	2	
Damage states are:	<input checked="" type="checkbox"/> ordered; <input type="checkbox"/> mutually exclusive; <input type="checkbox"/> simultaneous	
Author and date:	J Osteraas, H Krawinkler, B McDonald, J Hunt; December 2010	
Damage states, fragilities, and consequences		
	DS1	DS2
Description:	Cracking with offset > 1/16"	Toppling of all or portion
Illustration:		
Median demand (θ):	0.35g	0.5g
Total dispersion (β):	0.6	0.6
Repairs required:	Rebuild above break or replace entire chimney ¹	Rebuild above break or replace entire chimney ¹
Possible consequences:		
Repair cost (Y/N/?):	Y	Y
Death, injury (Y/N/?):	N	Y
Inoperative (Y/N/?): ²	N	N
Red tagging (Y/N/?)	N - "Area unsafe" tag	N - Possible "area unsafe" tag
Comments: ¹ Rebuilding with masonry will restore chimney to its pre-earthquake condition. Some jurisdictions prohibit unreinforced reconstruction and require either replacement of damage portion with a metal flue within a woodframe chase or complete removal of existing fireplace and chimney and replacement with code compliant reinforced masonry. ² Chimney and fireplace inoperative, portions of building beyond fall zone remain operative.		

Table 2. Supporting information summary

Introduction

It is axiomatic that masonry chimneys are one of the most fragile building components. Virtually all post-earthquake reconnaissance reports mention significant numbers of damaged or toppled chimneys. For example, following the recent New Zealand EQ, it has been reported that 14,000 chimneys were damaged or destroyed. City of Los Angeles records for the Northridge EQ identify approximately 30,000 chimneys for which repair permits were issued while other sources report a total of 60,000 damaged chimneys. While these data reinforce the fragile nature of masonry chimneys, like most field data reviewed, there are no data on the number of chimneys that were *undamaged*. A number of studies do report the number of damaged as well as undamaged chimneys within a portion of the area affected by the earthquake, though the data sets are quite small, especially for higher intensities of ground shaking. There are no published data regarding rates of chimney damage in areas of lower intensity of ground motions. Thus, little of the available data are useful for developing fragility functions.

Unlike other building components which are generally standardized, construction of residential chimneys is typically based on regional practices and artistry of masons as opposed to standard designs, engineered or not. Prescriptive design features have made their way into building codes over the decades, but even these (e.g., nominal steel reinforcement, anchorage to diaphragms) are often not explicitly designed, employ questionable construction detailing and are of highly variable construction quality. Not surprisingly, implementation of these prescriptive requirements has resulted in mixed improvement of seismic performance of chimneys. Neighborhoods of similar construction can exhibit not only a wide range of damage severity, but also a seemingly endless number of damage modes. As a consequence, the response of this seemingly simple component is in reality quite complicated: First, one cannot rely on the strength or ductility of key components such as mortar, wall or roof ties, reinforcing bond/development, etc. Second, the onset of substantial nonlinearity associated with first cracking and onset of rocking or sliding of all or part of the chimney can occur at low intensity and early in the ground shaking record. For instance, the restoring moment of a cracked, free-standing chimney acting as a rocking rigid block decreases as block rotation increases. In addition, incorporation of stiffness and strength degradation due to rocking, mortar crushing, damage to adjacent framing, etc., is difficult, at best, to model realistically.

Demand Parameter

Numerous demand parameters were considered. Based on simple mechanics, chimney cracking should be well correlated with PGA while toppling is best correlated with PGV. Some authors have suggested relationships based on PGV/PGA. Analytical results of this study showed better correlation with PGV than PGA, while both showed equally poor correlation with field data. Spectral acceleration at 0.3sec and 1.0sec were considered but did not improve correlation with field data. Some observed chimney failure modes are clearly related to story drift (including the “cripple story” between a foundation and a raised wood floor) but these failure modes are not common and the damaging story drift cannot easily be defined.

PGV and PGV/PGA were rejected as neither is readily available as a hazard parameter. Given the lack of a clearly better demand parameter and considering the universal availability of PGA, it was selected as the most practical demand parameter for chimney fragility analysis.

Damage States

Numerous chimney damage states are observed following earthquakes, ranging from complete collapse to damage that can only be identified by careful inspection of the chimney. Available data sets contain little information on the nature of the chimney damage observed. After considerable effort to develop fragility functions for various chimney configurations for multiple damage states using either empirical data or analytical studies, it was concluded that neither approach would provide defensible fragility functions. Rather, a hybrid approach based on professional judgment informed by the insight gained from analysis of empirical data and numerical simulation of chimney response was adopted to develop fragility functions for two damage states (cracking with visible offset and toppling of a portion of the chimney). DS1 captures those conditions where damage would be readily apparent (i.e. visible cracking, leaning of the chimney away from the building), likely result in a Yellow Tag – Area Unsafe, and require removal or replacement. DS1 does not include damage that can only be identified with a detailed inspection of the chimney. Thus, subtle damage is not reflected in the statistics for DS1. DS2 captures all toppling damage that has potential for human injury or death.

Empirical Data

As discussed above, while widely reported following every earthquake, there are few published post-event surveys that present chimney damage statistics in sufficient detail to provide a basis for development of fragility functions. Seven such useful data sets are discussed below. While not quantitative, two additional reports with relevant observations are summarized.

Notes on presentation of empirical data: Plots of empirical data points and fitted fragility functions are presented below, first for the individual data sets, then for combined data sets. The maximum likelihood curve fitting algorithm was provided by *Baker and Zareian (2009)*. The following must be considered when interpreting those plots:

- Individual data points may represent any number of observations, ranging from one to several hundred. The solver routine weights each data point to accurately reflect the actual number of observations in the fitted log-normal curve.
- An additional number of undamaged chimneys, equal in number to 1000 times the size of the dataset, was added to each dataset at an IM of 0.05g to reflect the fact that a very high percentage of chimneys in areas of low PGA would not be damaged, but the non-damaged data would not be included in any dataset because properties in areas of low ground shaking intensity were not surveyed. The addition of these “zero” data points has the effect of anchoring the fragility function close to zero probability of failure at very low IMs.

Santa Rosa Earthquake (1969): A field study of chimney damage over an area of 425 city blocks of mostly residential construction following the 1969 Santa Rosa EQ was conducted by *Steinbrugge et al (1970)*. The surveyed area extended well beyond the area of most intense shaking. Many of the woodframe dwellings (59%) were constructed post-1940, and “were more likely to include reinforcement for earthquake resistance, as opposed to the unreinforced masonry, pre-1940 construction.” Steinbrugge made several significant observations:

- Chimney damage for pre-1940 buildings was about three times more frequent than for post-1940

construction. This is attributed to higher quality construction, including use of steel reinforcing.

- Many of the damaged chimneys were broken at the roof line, most likely due to the presence of high demand (interface with house) and the presence of flashing creating a weak plane. Another common damage mechanism was rigid chimney rotation and separation from the more flexible house.
- Damaged chimneys were clustered in distinct, local geographic pockets, which were concluded to be the result of local changes in geology and shaking intensity.
- Of the pre-1920 homes, 18 chimneys were so severely damaged that they were considered total losses, while 11 were damaged but repairable; of the 1920-1940 homes, 8 chimneys were total losses and 1 was repairable; none of the chimneys of 1940-1969 vintage homes were observed to be damaged.

San Fernando (1971): Following the 1971 San Fernando EQ, *Scholl (1974)* conducted damage surveys of 1,043 mostly residential buildings in two areas of the City of Glendale. Virtually all buildings surveyed were more than 20 years old and large percentages (69% and 84% in the two areas) were greater than 40 years old. Of those, 610 had chimneys, of which 212 were damaged. For chimneys, the classification of “damage” was binary – no detail on the nature or extent of damage to chimneys (including fireplaces) was collected or reported. Data were collected in two areas – hillside and flatland, for which the main shock ground motions were estimated based on a nearby permanent strong motion instrument and aftershock records from two satellite strong motion instruments. Thus, two chimney damage ratio data points were presented. Using an effective spectral acceleration value as his ground motion parameter, Scholl found a marked difference between ground motions in the two areas (0.97g vs 0.54g). PGA values from ShakeMap are essentially identical for both sites at 0.29g. Using a PGA value of 0.29g and Scholl’s damage ratios yields the fragility curves shown in Figure 1.

Limitations of study/data: With respect to chimneys, the data includes chimney damage observed by the study team from the outside as well as interviews with building occupants regarding interior damage. Thus, the data likely includes all visible exterior damage as well as what could be very minor or pre-existing interior damage reported by building occupants. The report noted that occupant statements were taken at face value and no effort was made to ascertain a cause and effect relationship between the earthquake and reported observations. Thus, the data may overstate the damage, resulting in apparently more fragile chimneys. No information was available regarding the nature and extent of chimney damage nor the type and quality of the chimney.

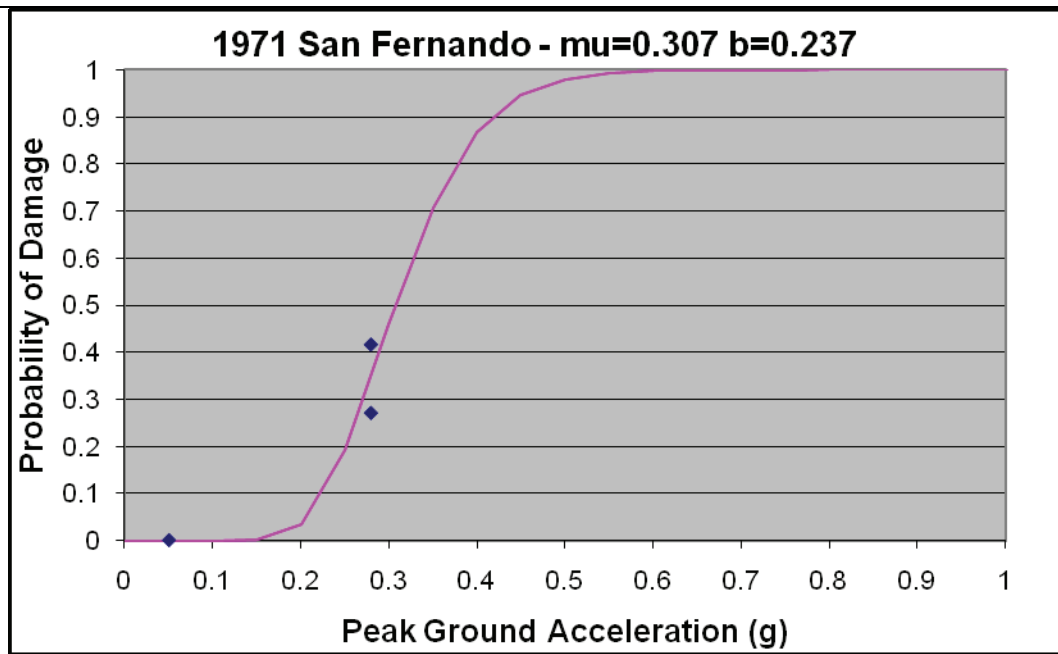


Figure 1. Fragility functions for 1971 San Fernando based on 2010 ShakeMap PGAs and damage statistics reported by Scholl (1974).

After the San Fernando EQ Earthquake, Steinbrugge et al (1971) surveyed 12,037 woodframe, single family dwellings affected by the ground shaking (almost 5% of 300,000 homes in the area). Almost all of these houses were reportedly constructed in last two decades (>1950); only 5.3% of the surveyed buildings were constructed before 1940. The field inspectors recorded chimney damage, and focused on some of the hard hit areas. Steinbrugge offers several significant observations:

- Wood buildings did very well; chimney reinforcement in the more modern vintage houses “vastly reduced” chimney damage.
- Newer houses did better than older; one story did better than two story
- Of 12,037 homes, 67.6% had no chimney damage, while 16% exhibited slight damage, 6.6% moderate, and 7.4 % severe.
- The 7.4 % of chimneys exhibiting severe damage were almost entirely composed of the 5.3% of the homes constructed before 1940.

Steinbrugge concluded that had the vast majority of these chimneys not been reinforced, then the “no damage” category would have been closer to 0% rather than 67.6%. Damage was found in local pockets, thought to be most likely related to local geological features affecting the ground shaking intensity.

Limitations of study/data: Insufficient data published to permit development of fragility functions.

Northridge (1994)-a: For the 1994 Northridge EQ, two sets of data on chimney damage are publically available. *ATC-38 (1994)* conducted a systematic survey of about 500 buildings located within 1,000 feet of 31 strong-motion recording stations with PGAs ranging from 0.13g to 1.78g located throughout the greater Los Angeles area. The project report included a CD with all survey data and a picture for each property, making independent analysis of the data relatively straightforward. The dataset includes 233 buildings with chimneys of which 57 were identified with some degree of damage. In many cases, qualitative comments regarding the nature of chimney damage were included, though there is no apparent consistency between inspectors regarding chimney damage characterization. Selected ground motion

data for the 31 stations was presented in the report, while time history data and response spectra were contained on the CD. Additional ground motion data can be found in Appendix A of *King et al (2005)*. One of the stations used in the study was the Cedar Hill Nursery station in Tarzana, with a recorded PGA of 1.78g. That value reflects local amplifications and is not representative of surrounding ground motions. Accordingly, the value used for the present study was reduced from 1.78g to 0.40g. Data points and the fitted fragility function are presented in Figure 2.

Limitations of study/data: Field inspection methodology and damage classifications for chimneys are not described. There are few chimney damage data points in areas of higher accelerations which make the data for those areas suspect, a general observation made by King regarding building damage in general. No information is provided regarding type of chimney, condition, or quality of workmanship.

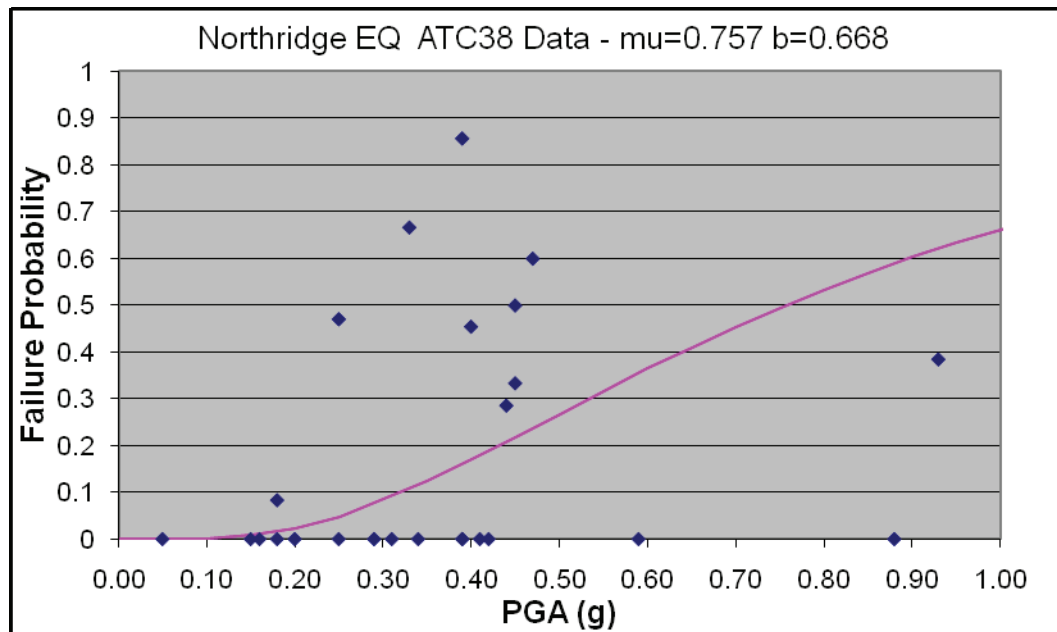


Figure 2. Fragility functions for chimneys based on Northridge EQ data as reported in ATC-38 (1994).

Northridge (1994)-b: Following the Northridge EQ, *Graf (2009)* assembled data from detailed inspections of 225 residential properties, 157 of which had chimneys. Roughly one-third of the chimneys were constructed before 1940. Graf's data points (less a single observation with a reported PGA>1.0g) and the fragility function fitted to those data points are presented in Figure 3.

Limitations of study/data: Damage classification is binary – no information was provided regarding the type or extent of damage. Data does not reflect a random selection, as only properties with reported earthquake damage were inspected. No information is available regarding configuration, type of construction, or construction quality.

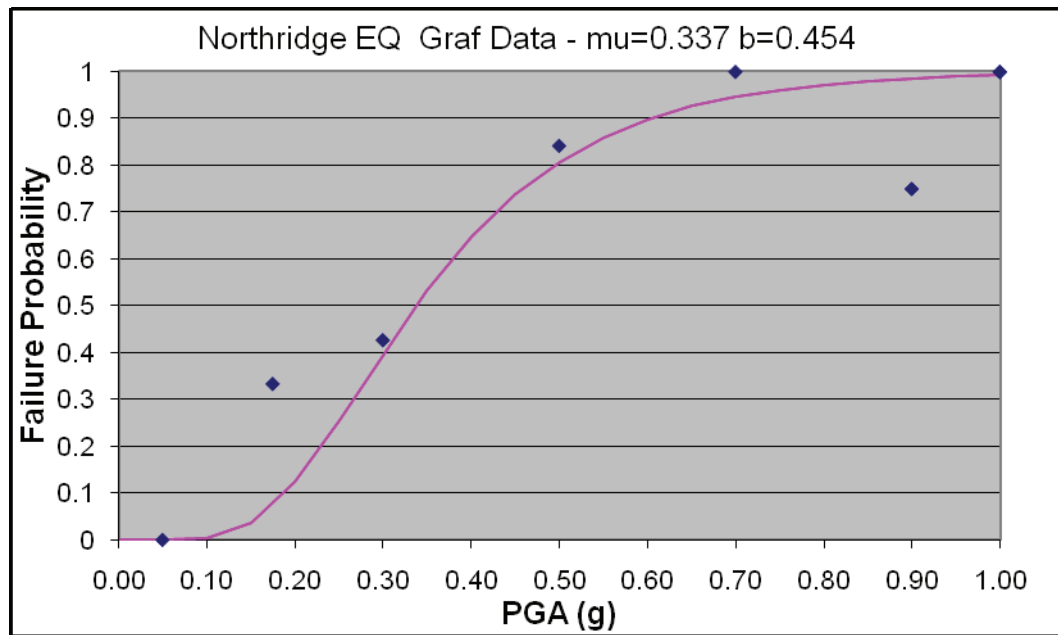


Figure 3. Fragility functions for chimneys based on Northridge EQ data as reported by Graf (1994).

Northridge (1994)-c: Following the Northridge Earthquake, the City of Los Angeles Department of Building Inspection (*LADB&S 1994*) tracked repair permits and coded different types of repair and structure types. Within their data are 29,536 permits for chimney repair only. Based on the observations of *Steinbrugge (1970)* the chimneys in the LADB&S dataset were, overwhelmingly, reinforced and anchored to the floor and roof diaphragms. Yet, the dataset can be used to extrapolate fragility functions for unreinforced masonry chimneys. Based on PGA grid points in the ShakeMap archive of Northridge EQ ground motions, each of the 29,536 chimneys in the dataset were assigned a site-specific PGA value. An empirical cumulative probability distribution of damage was calculated by dividing the cumulative number of repairs by *an estimate of* the total number of masonry chimneys in the affected area. The number of masonry chimneys was based on adjusting the total number of detached, single-family dwellings. The number of affected dwellings came from Los Angeles Department of Water and Power water meter data, which provides the total number of single-family detached dwellings in each zip code for which there were chimney repair permits. The number of dwellings was adjusted downward to reflect the number of masonry chimneys by the ratio of all houses to houses with chimneys (USGS), and the ratio of the total number of damaged chimneys to those for which permits were pulled (various references quote estimates of 60,000 badly damaged chimneys). In addition, the probability of failure was increased by a factor of three per Steinbrugge's observed damage rates for reinforced and unreinforced chimneys. The extrapolated data and fitted lognormal distribution are presented in Figure 4.

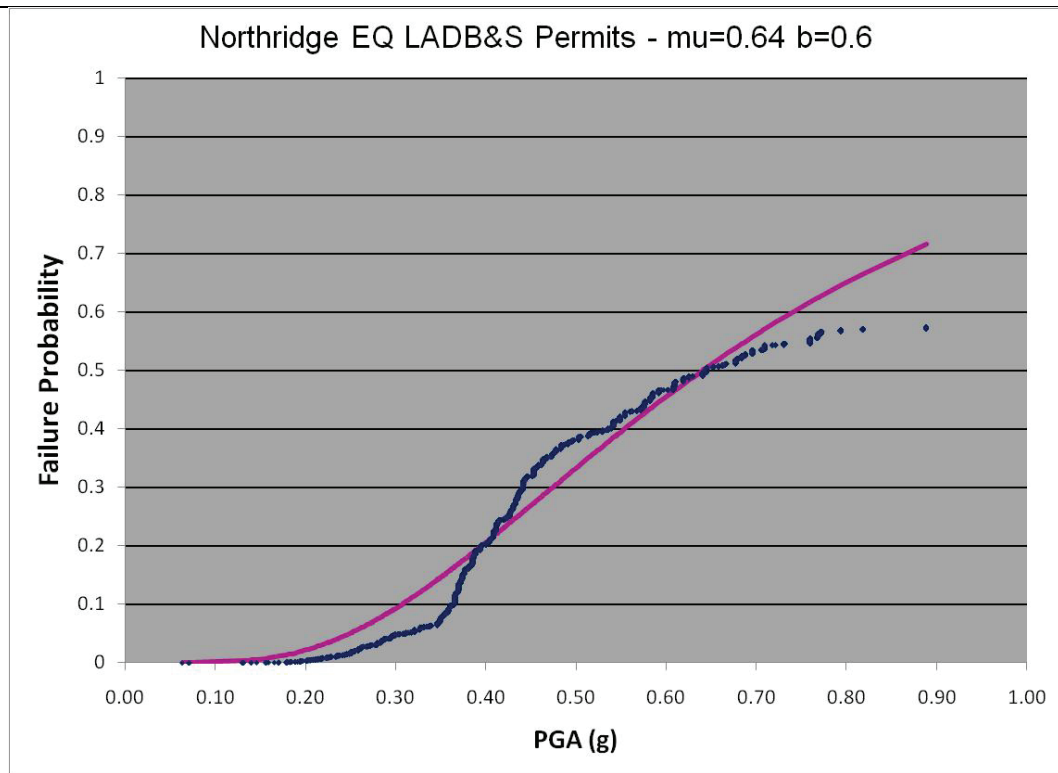


Figure 4. Fragility functions for unreinforced masonry chimneys extrapolated from LADB&S dataset of Northridge EQ chimney repair permits.

Nisqually (2001)-a: While several reports on the 2001 Nisqually EQ reference chimney damage, derivation of defensible fragility curves is virtually impossible. *Booth et al (2001)* conducted a systematic windshield survey (using binoculars) of approximately 60,000 chimneys over 50km² and identified 1,556 damaged chimneys. The objective of their survey was not to study chimney damage as such but to identify pockets of damage corresponding to geological features, using observed chimney damage as an indicator of shaking intensity. Data recorded for damaged chimneys consisted of GPS coordinates and three classes of damage (small cracks, large cracks/partial collapse, chimney partially or totally destroyed). Minor damage and hidden damage was not recorded. The total number of chimneys in an area was determined from analysis of air photos. A fragility curve based on reported failure rates and PGAs in

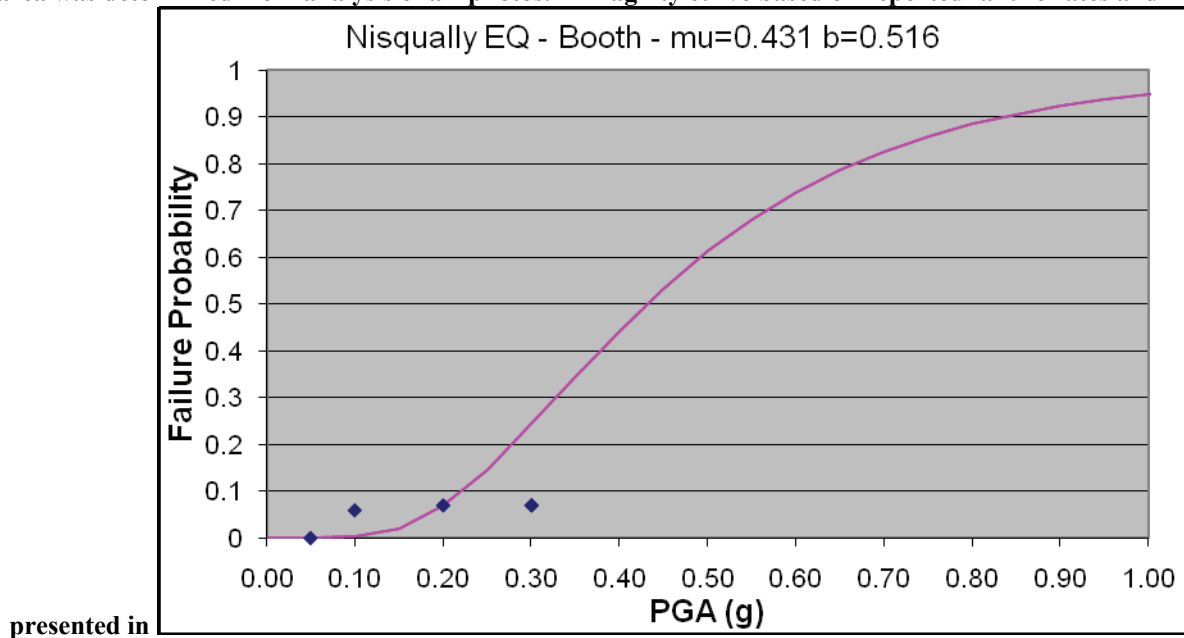


Figure 5.

Limitations of study/data: Only summaries of the full survey were available, not the actual data. Rates of occurrence of the three damage states cannot be extracted from the summary data available. No information is available on age, configuration, type of construction, or construction quality.

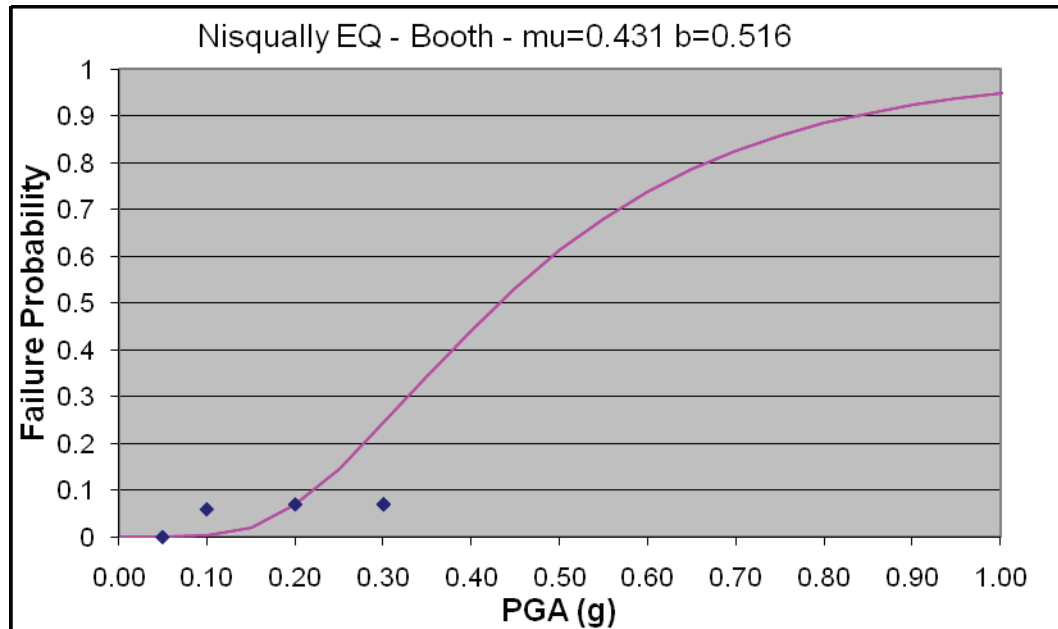


Figure 5. Fragility function for chimneys in the Seattle area based on Nisqually EQ damage observations as reported by *Booth et al (2002)*.

Nisqually (2001)-b: Following the Nisqually EQ, *McMullin et al (2001)* surveyed 120 houses in an Olympia neighborhood just east of the capitol grounds. 84 chimneys were observed, of which 28 had visible damage. ShakeMap indicates a PGA of 0.16g in the surveyed neighborhood.

Limitations of study/data: No information is available regarding nature or extent of damage, configuration of chimney, quality of construction, or age.

San Simeon: Sanitized (i.e. containing no property identification) chimney survey data for the San Simeon EQ were obtained from the California Earthquake Authority (CEA). The data set included 97 masonry chimneys on 90 dwellings, of which between 20 and 27 had reported damage. Entries for damaged chimneys also included their repair cost, though there is not information whether one or multiple chimneys at a dwelling were damaged. The data set also includes the site PGA derived from ShakeMap, year of construction and number of stories.

Limitations of study/data: No information beyond repair cost on the nature or extent of reported damage, chimney configuration, or quality of construction.

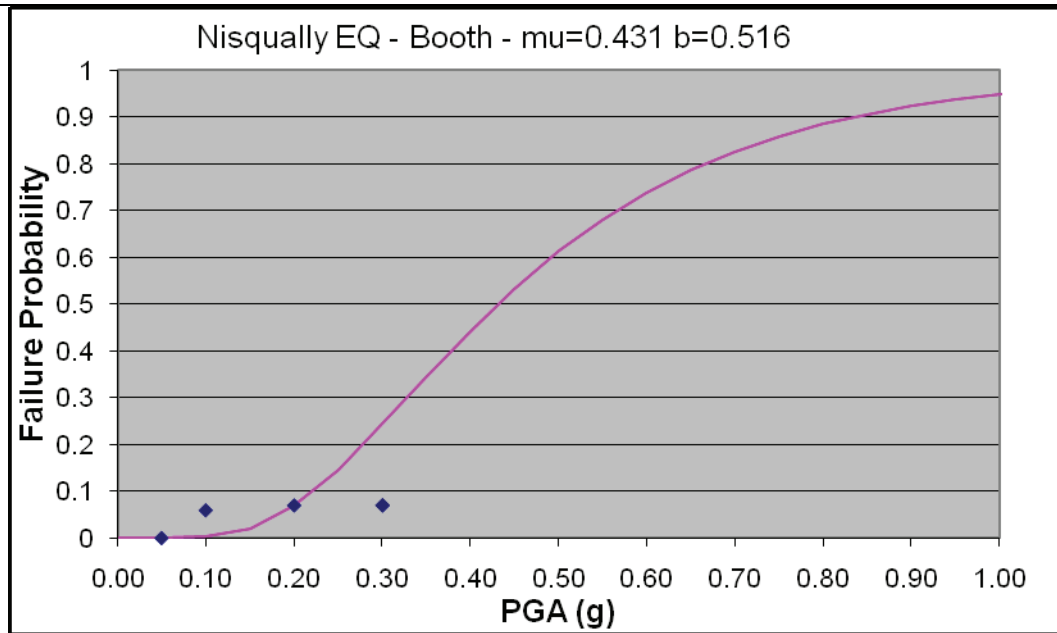


Figure 6. Fragility function for chimneys in the San Simeon area based on earthquake insurance claims underwritten by the CEA.

Summary: To generate fragility curves incorporating data from as many sources as possible, all data sets based on inspections of individual chimneys with a well defined denominator (i.e. those described above) were combined into a single dataset as shown in Table 1. Given the large size of the Booth dataset for the Nisqually EQ and serious concerns about the validity of the data, especially with respect to the denominators, both numerators and denominators in Booth's dataset were divided by 100 before entering into the combined dataset. All data points except Booth's are plotted in Figure 7 along with the fitted fragility curve. Figure 8 is identical to Figure 7, with the addition of Booth's. Even with a two order-of-magnitude reduction in size, the Booth dataset comprises about one-fifth of the total dataset.

Table 1. Combined empirical dataset

Source	PGA (g)	Sample Size	# Damaged	Comments
San Fernando - Scholl	0.28	285	77	
San Fernando - Scholl	0.28	325	135	
NREQ - ATC-38	0.15	10	0	
NREQ - ATC-38	0.16	3	0	
NREQ - ATC-38	0.18	1	0	
NREQ - ATC-38	0.18	12	1	
NREQ - ATC-38	0.20	11	0	
NREQ - ATC-38	0.25	1	0	
NREQ - ATC-38	0.25	17	8	
NREQ - ATC-38	0.29	1	0	
NREQ - ATC-38	0.31	1	0	
NREQ - ATC-38	0.33	6	4	
NREQ - ATC-38	0.34	1	0	
NREQ - ATC-38	0.39	8	0	
NREQ - ATC-38	0.39	7	6	
NREQ - ATC-38	0.39	4	0	
NREQ - ATC-38	0.41	7	0	

NREQ - ATC-38	0.42	2	0	
NREQ - ATC-38	0.44	7	2	
NREQ - ATC-38	0.45	14	7	
NREQ - ATC-38	0.45	3	1	
NREQ - ATC-38	0.47	15	9	
NREQ - ATC-38	0.59	7	0	
NREQ - ATC-38	0.88	20	0	
NREQ - ATC-38	0.93	26	10	
NREQ - ATC-38	0.40	11	5	Reported as >1.78g
NREQ - Graf	0.18	3	1	
NREQ - Graf	0.30	82	35	
NREQ - Graf	0.50	19	16	
NREQ - Graf	0.70	8	8	
NREQ - Graf	0.90	8	6	
NREQ - Graf	1.00	1	1	Reported as >1g
Nisqually - Booth	0.1	124	7.39	0.01 x actual count
Nisqually - Booth	0.2	116	8.13	0.01 x actual count
Nisqually - Booth	0.3	10.8	0.76	0.01 x actual count
Nisqually - McMullin	0.16	84	28	
San Simeon - CEA	0.12	20	2	
San Simeon - CEA	0.21	22	3	
San Simeon - CEA	0.28	40	10	
San Simeon - CEA	0.34	17	4	
San Simeon - CEA	0.44	1	1	
Total		1361	396	

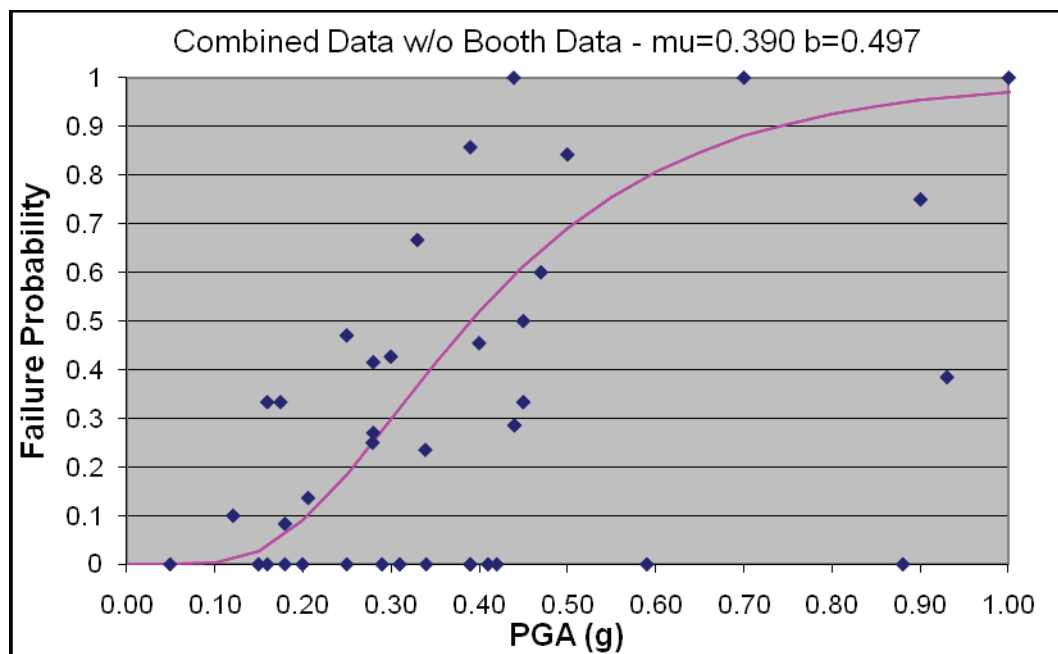


Figure 7. Fragility function for chimneys based on inspection data following San Fernando, Northridge, Nisqually (including McMullin, excluding Booth), and San Simeon.

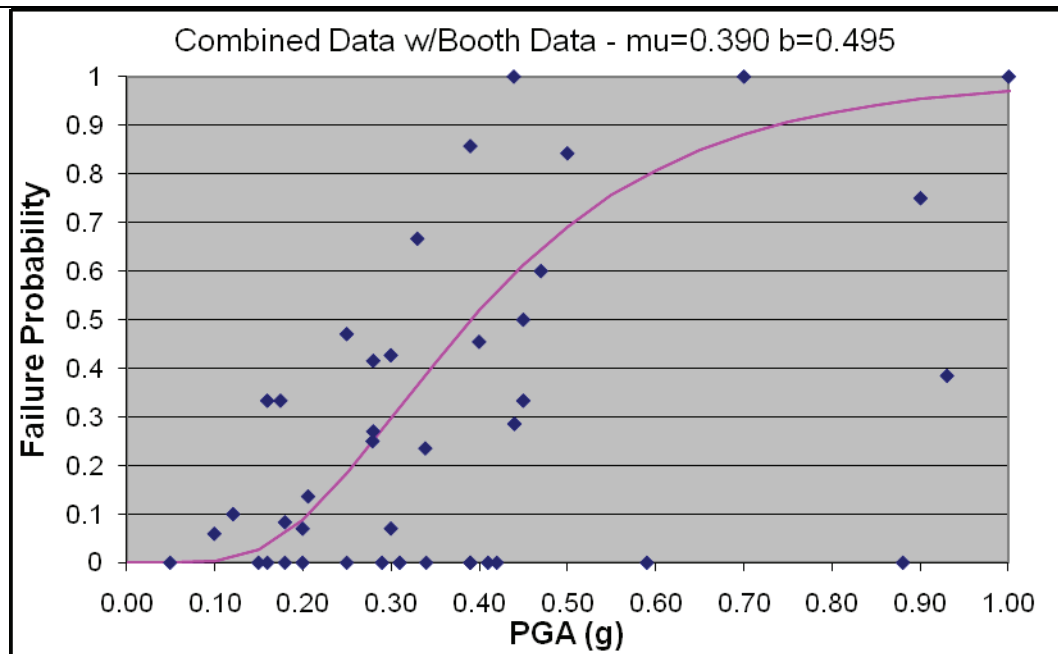


Figure 8. Fragility function for chimneys based on inspection data following San Fernando, Northridge, Nisqually (McMullin & Booth x 0.01), and San Simeon.

Data from Analytical Studies

Cape Ann (1755): *Whitman (2002)* developed theoretical damage state probabilities for chimneys in the Boston area after the 1755 Cape Ann EQ as shown in Table 2.

Table 2. Theoretical damage state probabilities for chimneys (*Whitman 2002*)

Damage State	$a/g = 0.05$	$a/g = 0.075$	$a/g = 0.10$	$a/g = 0.125$
None	0.70	0.50	0.30	0.20
Minor cracking	0.15	0.25	0.30	0.25
Shattered, etc.	0.15	0.25	0.40	0.55

Utilizing the most severe of the three damage states identified by Whitman (shattered, etc.), *NAHB (2003)* developed fragility functions as shown in Figure 9.

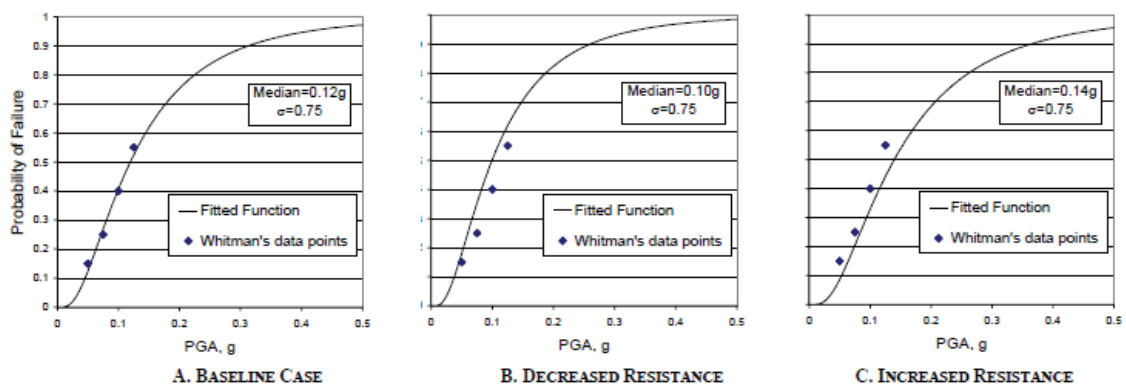


Figure 9. Fragility functions for brick chimneys modeled with cumulative lognormal distribution (*NAHB 2003*).

Limitations of study/data: Considering the significant changes in building and chimney construction materials and practices since 1755 (e.g. concrete rather than rubble foundations, portland cement rather than lime mortar), *Whitman's* data provides perhaps a lower bound on the performance of modern chimneys but does not appear to be applicable to “modern” buildings.

Review of analytical studies. Many analytical studies have been performed in the past 50 years on rocking and overturning of rigid blocks. Most studies do not address explicitly the combination of rocking plus sliding, but much of the past work may be applicable to the response of masonry chimneys after initial cracking at the base, shoulder or roof line. An early and important study of the rocking of rigid blocks by *Housner (1963)* explored anomalous damage observations after several earthquakes, namely, the survival of tall slender monuments and structures in areas where their squat and apparently stable counterparts were severely damaged. Housner investigated rocking of rectangular blocks on rigid bases undergoing constant, sinusoidal and earthquake ground motions. His key results included analytic expressions for the effective period of rocking, which tends to infinity as the rocking angle approaches the point of imminent overturning. Also, Housner showed that there is a size effect, that is, the propensity for overturning is not governed solely by aspect ratio, and that dynamic survival is not predicted by simple statics.

Since Housner's paper there have been many researchers who have advanced this topic: we identify a few here, but acknowledge this is by no means an exhaustive list. *Alsam et al (1980)* carried out a series of shake table tests of rigid block rocking and showed that the response is very different from classical structural systems. In fact, the response of the block was so sensitive to input parameters that experimental results using earthquake ground motions were not repeatable, much less predictable. *Ishiyama (1982 and 1984)* developed a computer program to simulate the response of a rigid block that included rocking, sliding, and jumping, alone and in combination. Through analysis and testing, he showed that any criterion for overturning needs to include both peak acceleration and peak velocity, and provided expressions for predicting overturning failures. *Yim, Chopra, and Penzien (1980)* also showed through numerical simulation that the response of a rigid block is very sensitive to block size, aspect ratio and characteristics of the ground motions. While individual responses could differ, they showed that in a probabilistic sense the vulnerability to overturning increases with aspect ratio and motion intensity, and decreases with block size. Their paper provides plots showing cumulative probability distributions for overturning as a function of ground motion intensity measures, based on numerical simulation using synthetic ground motions. *Spanos and Koh (1984)* defined the governing differential equations for rocking blocks and used numerical integration to show, among other things, combinations of frequency and amplitude that lead to overturning for differing block aspect ratios. More recently, *Sharif et al (2007)* and *Meisl et al (2007)* have investigated probabilistic failure criteria for rocking of block walls with anchorage to diaphragms.

Purvance et al (2008) used Monte Carlo simulations and logistic regression analysis to quantify overturning fragilities of a rigid block subjected to earthquake-like random vibration waveforms. Their primary configuration variables were the aspect ratio B/H and the frequency parameter $p = \sqrt{(mgR/I)}$, and their primary demand variables were PGA and the ratio PGV/PGA. They also performed shaking table tests to calibrate their results. From the plots presented in their paper, it is estimated that the median overturning capacity, expressed in PGA, for the range of PGV/PGA ratios from about 0.05 to 0.20 varies from about 0.75g to 0.35g. The capacity clearly decreases with an increase in the PGV/PGA ratio, demonstrating the importance of velocity pulses.

In summary, these studies verify the large expected scatter in the response of block-like structures (such

as chimneys and parapets) to earthquake ground motions, and the lack of deterministic equations available for predicting toppling damage – much less many of the other potential chimney and parapet damage modes.

From past work, and from mechanics principles, it becomes clear that toppling and sliding of chimneys depend on geometric and material parameters and boundary conditions, as well as on the frequency characteristics of the input motion. In the simplest idealized case a chimney could be represented by a single rigid block subjected to rocking (defined by θ) and sliding (defined by δ) as illustrated in Figure 10.

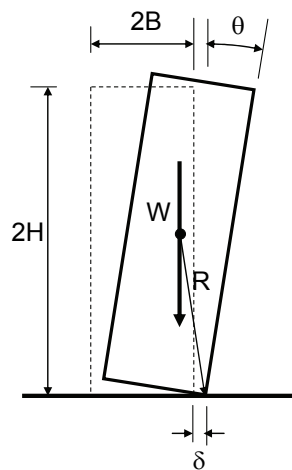


Figure 10. Rocking and sliding of rigid rectangular block.

The response of this idealized rigid body depends on the following parameters (and others not itemized here):

- Dimensions B and H (aspect ratio H/B);
- Size and mass (or weight W);
- Frequency parameter $p = \sqrt{(mgR/I)}$;
- Coefficient of restitution;
- Coefficients of static and dynamic friction;
- Peak ground acceleration (PGA), relevant for uplift;
- Peak ground velocity (PGV) and pulse characteristics of ground motion; and
- PGV/PGA ratio.

Using these parameters in analytical predictions of sliding and toppling, fragility curves do not consider variations in boundary conditions and material properties such as mortar crumbling that will reduce the effective width ($2B$) of the rigid blocks. These variations will have to be accounted for by an increase in the dispersion. Moreover, variations in ground motion characteristics cannot be incorporated comprehensively in an analytical fragility curve prediction. To overcome this shortcoming, it was decided to use a single but comprehensive set of ground motions in order to account for record-to-record variability. The approach employed here has been used in other ATC projects, such as ATC 63, i.e., FEMA P695, in which record-to-record variability is accounted for by using a relatively large set of representative ground motions, and modeling uncertainties are accounted for by inflation of the dispersion. This approach is employed in the Working Model 2-D study summarized below.

The following pilot study was performed to explore whether the Working Model 2-D study will provide

results that are in line with expectations based on simple mechanics principles.

For overturning, consider the rigid block shown in Figure 10. At the onset of lift-off ($\theta=0$), the horizontal force F required for equilibrium is $W*B/H$. If F is considered to be an equivalent static load, the onset of block rotation is imminent when the acceleration reaches a critical value A_c , i.e.,

$$A_c = \frac{B}{H} g \quad (1)$$

This equation, i.e., $PGA = A_c$, can serve as a simple fragility value for initial uplift.

For toppling, an inertial overturning moment must be sustained for some time before the critical angle ($\theta_c = \tan^{-1}(B/H)$) is attained and toppling proceeds under the force of gravity alone. Yim et al (1980) provided expressions for duration required to achieve overturning for sinusoidal and square acceleration pulses. However, as noted in the reference, toppling is a function of the time history and could occur at smaller accelerations / shorter durations depending on the characteristics of the ground shaking. The criterion for overturning can be based on energy principles: Consider a block moving laterally with velocity V that suddenly comes to a stop. For sufficiently high V , the sudden stop will cause the back corner to uplift, raising the center of gravity (potential) of the block. By equating the kinetic energy of the moving block to the increased potential when the block rotates to the critical angle θ_c one can show that:

$$V_c = \sqrt{2gR(1 - \cos\alpha)} \text{ where } R = \sqrt{H^2 + B^2} \text{ and } \alpha = \tan^{-1} \frac{B}{H} \quad (2)$$

This equation, i.e., $PGV = V_c$, can serve as a simple fragility value for overturning (toppling).

To test how well Equation 2 predicts overturning of rigid blocks subject to the set of ground motions, three sizes / shapes of masonry block were analyzed using the dynamic simulation software Working Model 2-D. The blocks were modeled as rigid, resting on a rigid table surface that was accelerated horizontally to simulate 44 acceleration records (FEMA P695 record set). The ground motions were incrementally increased in amplitude in the time domain until overturning occurred and the PGV of the scaled ground motion were recorded. The peak velocity required to overturn a 30-inch-wide block of various height per Equation 2 is compared in Figure 11 to the average peak velocity of the FEMA P695 record, scaled until overturning occurs.

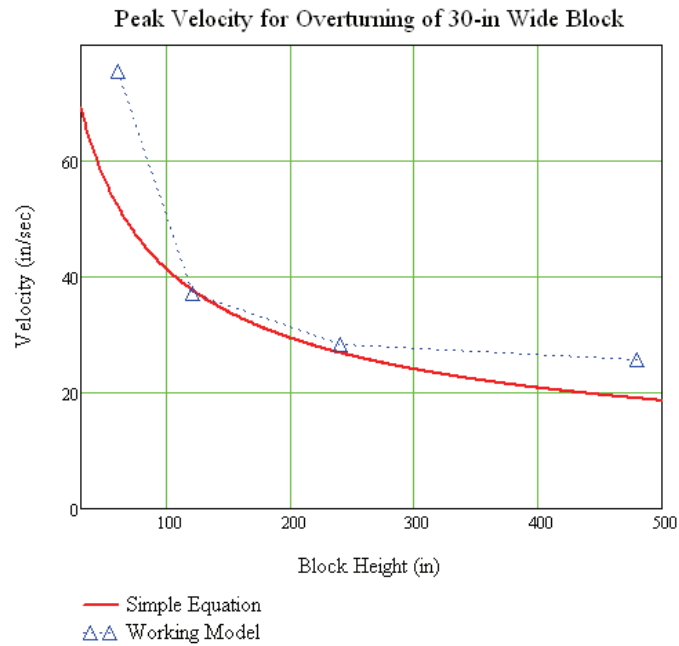


Figure 11. Peak velocity required to overturn 30-inch-wide block of varying height.

Results from Study with “Working Model 2-D”

Considering the disparity of results obtained in various analytical studies and the apparent sensitivity of the results to ground motion frequency characteristics, the need was evident for comprehensive simulations of chimney failure modes using actual ground motion records of sufficient intensity to trigger the postulated failure modes of sliding and toppling. This study focused on the response evaluation of free standing and anchored (rooftop) chimneys using the dynamic simulation software Working Model 2-D (*Design Simulation Technologies*). The software permits simulation of ground motion on a shaking table and representation of structures by means of rigid bodies and springs. Results from this program for wall rocking have been compared to experimental results of shaking table tests (*Sharif et al 2007*) and have provided accurate predictions of seismic response.

Two types of chimneys were investigated. A free-standing chimney that can be represented by a single rigid block resting on a rigid table surface, and a rooftop chimney attached to a house at the eave line. The house is represented by a single, hinged portal frame with large (relative to the chimney) mass and stiffness resulting in an undamped period of 0.1 seconds, and an explicit damper that results in 5% critical damping (Figure 12). The top of the frame is at 120 inches above the table, corresponding to the eave elevation of the benchmark case. In both cases the rigid table surface is subjected to a set of recorded horizontal ground motions in a manner summarized later.

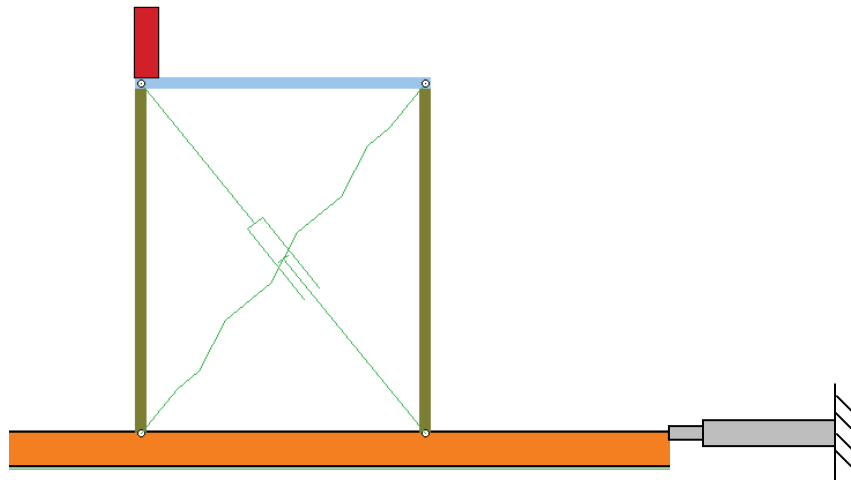


Figure 12. Rooftop chimney model used in Working Model 2-D.

The following properties of the chimney were used:

- Width $B = 24''$
- Height $H = 180''$, $228''$, and $132''$ (essentially representing mean and mean \pm sigma)
- Unit weight $= 120 \text{ lb/ft}^3$
- Coefficient of restitution $= 0.02$
- Coefficient of static and dynamic friction $= 0.8$ and 0.7

Arguments for the height dimensions are as follows: Assume ground-to-top-of-eave height of 120 inches. In average the chimney extends 60 inches above the height of the eave, resulting in a total height of 180 inches. This height is consistent with the 2006 International Residential Code, which requires a 10-foot clearance between the chimney wall and the roofing surface at an elevation 2 feet below the top of chimney. For a common 4:12 roof, this would require 5-foot, 4-inch extension - rounded herein to 5 feet. The taller chimney variant is based on the same considerations but for a 9:12 roof slope (steep but not rare), for which the IRC would require $2 + 10 \cdot (9/12) = 9$ -feet (rounded down), for a total chimney height of 228 inches. For a lower bound chimney height, relative to the benchmark, we assumed a total chimney height of 132 inches. For the rooftop chimney, the dimension to the top of the eve was kept constant at 120 inches and the upper block was taken as 60 inches and 108 inches respectively.

The coefficient of restitution appears to be small, but it provided the best match with experimental results reported in Sharif et al. (2007). Sensitivity studies did show that variations of this and friction coefficients had little effect on fragility curves.

The chimneys were subjected to the FEMA P695 (ATC-63) set of 44 ground motion records (actually 22 pairs of records). This record set is discussed in detail in FEMA (2009). The records represent ground motion recorded at sites greater than 10km from the fault rupture. The records are intended to represent an unbiased suite of motions associated with earthquake magnitudes between 6.5 and 7.9.

Incremental dynamic analysis (IDA) was performed for each record, whereby the intensity of the record was increased until “significant” sliding and then toppling occurred. The sliding capacity was defined as that ground motion intensity that caused sliding between chimney blocks or between the chimney and the

table of at least 1/16". Toppling was defined as overturning of a chimney block. It is acknowledged that definitions of these two failure modes involve simplifications, considering that a number of damage modes have been observed after recent earthquakes, including cracking at the base, shoulder or roofline; shifting at the base, shoulder or roofline; separation from the house structure; general disintegration (crumbling) of mortar and units; and overturning / toppling. Toppling commonly occurs at the roof line, but can also occur about the base when anchorage to the structure is poor or nonexistent.

Various intensity measures (IMs) associated with the two failure modes were recorded, among them peak ground acceleration (PGA), peak ground velocity (PGV), and spectral acceleration at $T = 1$ sec. ($S_a(1.0)$). The analysis results were post-processed by sorting each record by the IM value at the point of failure (sliding greater than 1/16" or toppling). The sorted records were used to assemble the empirical cumulative distribution functions (probability of failure given IM), and lognormal distributions were fit to the CDFs using least squares.

Results for free-standing chimney:

The chimney is assumed to be free-standing and not structurally connected to the house structure, which are reasonable assumptions for older vintage chimneys, or poorly constructed modern chimneys that have suffered cracking at the base and full partial detachment from the structure early in the time history. Sliding towards the house was not allowed, that is, the chimney was only allowed to slide in one direction.

Figure 13 shows sliding and toppling fragility curves for the average chimney height of 180", using PGA (bottom scale) and PGV (top scale) as intensity measure. Median (θ) and logarithmic standard deviation values are shown in the figure legend. The dispersion (β) for the PGV fragility curves is clearly smaller than that for PGA (0.35 versus 0.54 for toppling), indicating that PGV is a better intensity measure than PGA. Nevertheless, PGA is used as the pertinent intensity measure from here on because of its availability in seismic hazard maps. Moreover, the empirical data reported earlier did not show a clear preference of PGV over PGA in the fragility curves.

It is interesting to note that the ratio of median PGV to median PGA of the record set is 0.115, and the ratio of median toppling capacity given PGV to median toppling capacity given PGA is 0.111. This demonstrates consistency of the predicted toppling results. It also indicates that in the median it should not matter whether PGA or PGV is used as an intensity measure (demand parameter).

The median sliding capacity (intensity causing sliding) for the free-standing chimney is only about 20% smaller than the toppling capacity. This raises the question whether it is justified to distinguish between the damage states of sliding and toppling, considering also that observations made in earthquake reconnaissance documents rarely make a distinction between chimney damage states. The main argument for making a distinction between sliding and toppling is the life safety concern associated with toppling.

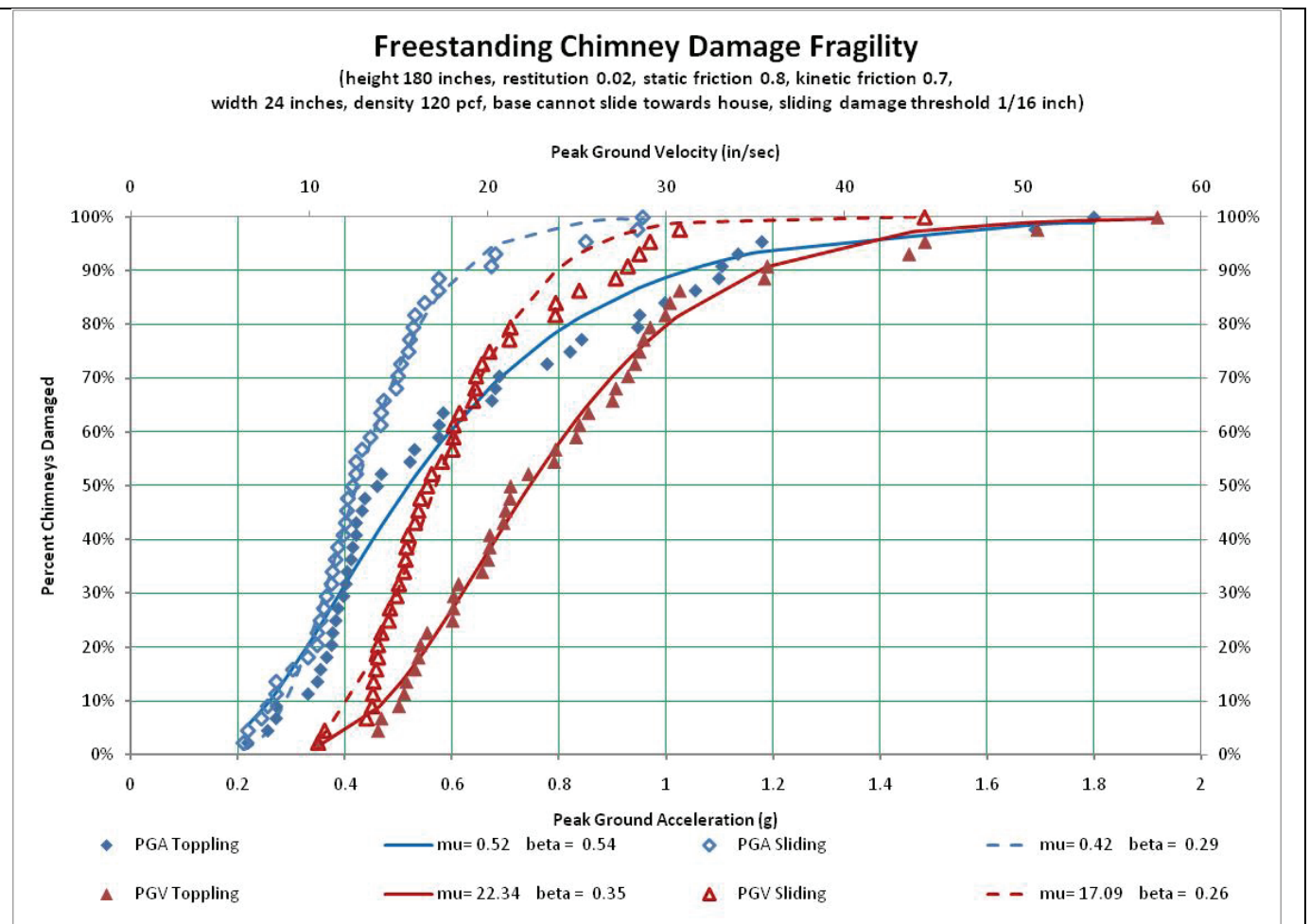


Figure 13. Sliding and toppling fragilities for freestanding chimney, PGA and PGV as IM.

The effect of chimney height on toppling fragility curves is shown in Figure 14. For the range of heights considered for the free-standing chimney, this effect is relatively small and can be accounted for by increasing the dispersion β by a small amount.

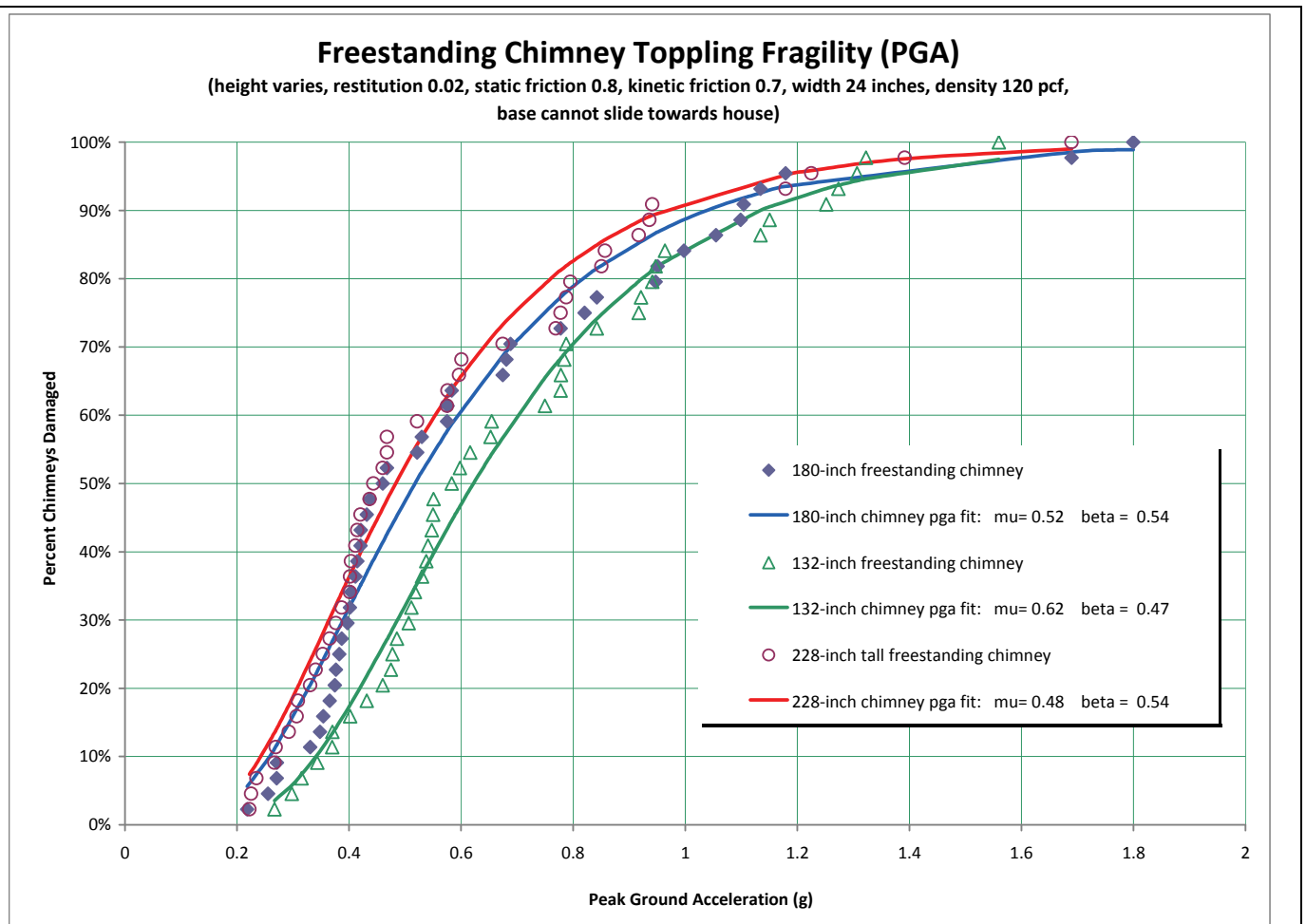


Figure 14. Toppling fragilities for freestanding chimneys of different height.

Based on the analytical results obtained here, and considering the uncertainties in the assumptions made for sliding and rocking of rigid blocks, it is recommended to use a median toppling capacity of 0.5g with a beta of 0.6. The results indicate a median sliding capacity of 0.4g with a beta less than 0.5. These values apply for free-standing non-engineered (without reliable reinforcement) chimneys that are not attached to the house and not affected by the motions of the house. It is reasonable to use the same values for non-engineered chimneys that are nominally attached to the house, but with an attachment that does not have sufficient resistance to prevent sliding or rocking.

Results for rooftop chimneys:

In this simulation it is assumed that the chimney attachment to the house is of sufficient strength and stiffness so that no relative translation can take place between the chimney and the house. The house has a natural period of 0.1 sec and a mass that is large compared to that of the chimney. Ground motion is imparted at the base of the house, and it is assumed that the house responds elastically. Because of the attachment, toppling and sliding can occur only at the eve level. This model captures damage related to the portion of the chimney extending above the roof line (perhaps the most common damage mode), and the chimney below is not included in the simulations.

Toppling fragility curves are presented in Figure 15 for “rooftop” chimneys extending by 60” and 108”, respectively, above the eave line, together with the fragility curve for the free-standing 180” chimney.

The attachment to the house causes a clear increase in median toppling capacity, but the increase depends strongly on the height of the chimney above the eve line. If this height is 60" (which results in a total chimney height of 180" if the eve height is 120"), the increase is about 60% compared to the free-standing chimney, but it is only about 25% if the above eve height is 108".

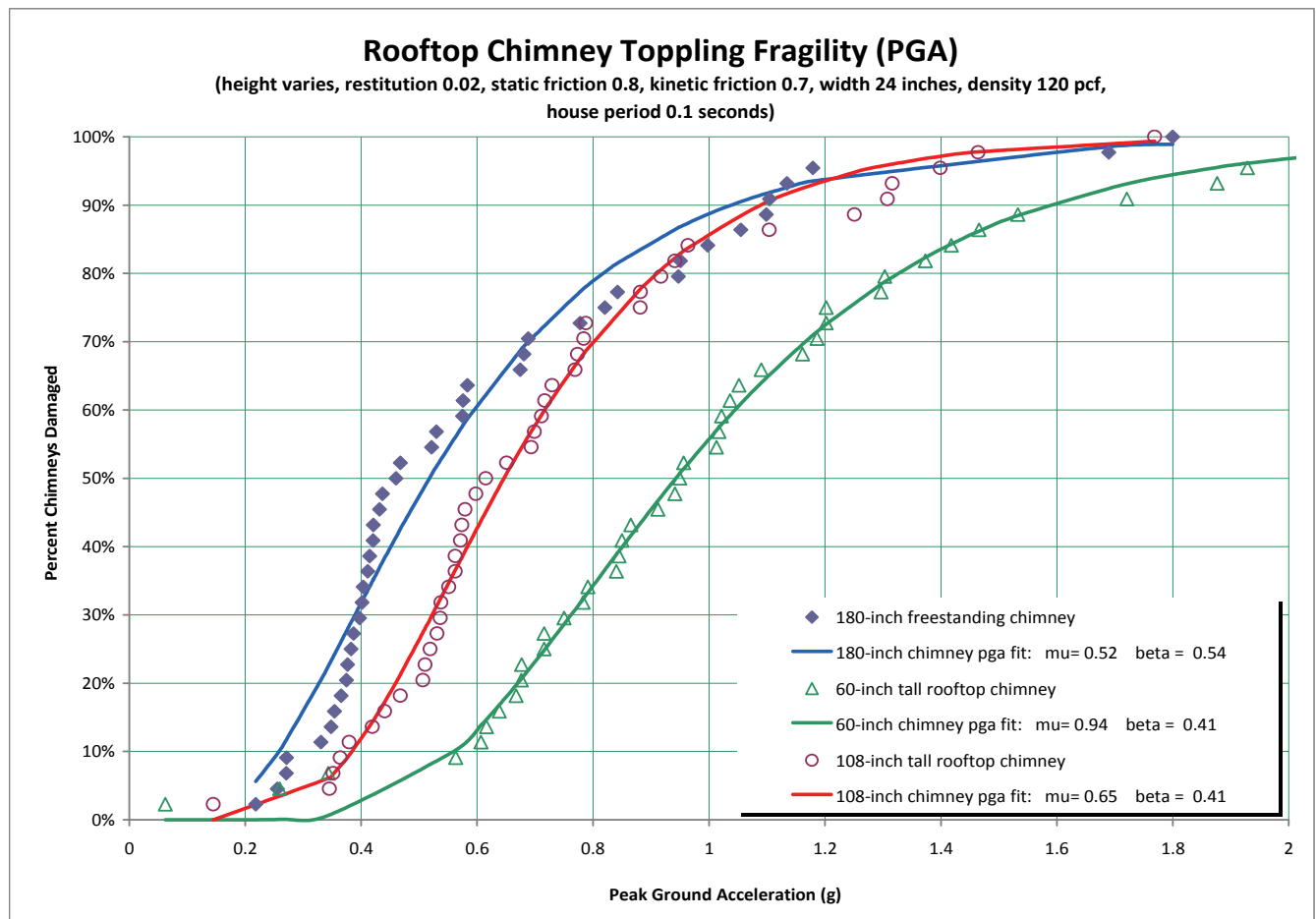


Figure 15. Toppling fragilities for rooftop chimneys of different height.

The sliding fragilities shown in Figure 16 indicate that sliding occurs at a lower PGA for an attached (or rooftop) chimney than for a free-standing chimney, and that the capacity is sensitive to the height of the chimney block above the roof line. This observation applies also for non-engineered chimneys that are restrained from movement at the ceiling or roof line. For this reason it is recommended to reduce the median sliding capacity for non-engineered chimneys from the value of 0.4 recommended for free-standing chimneys to a value of 0.35 and to increase the dispersion to 0.6. The observation that the sliding capacity decreases compared to a free-standing chimney is not surprising, because the maximum input acceleration imparted by the house to the rooftop portion of the chimney increases greatly compared to the PGA and overcomes the beneficial effect of a smaller aspect (H/B) ratio. The higher acceleration will cause early uplift, which in turn will cause early bouncing and sliding. This is much more evident in the 108" rooftop chimney block (H/B = 4.5) than the 60" block (H/B = 2.5). A mitigating condition is that for large PGAs the house is expected to respond inelastically, and very high roof accelerations are not very likely to develop.

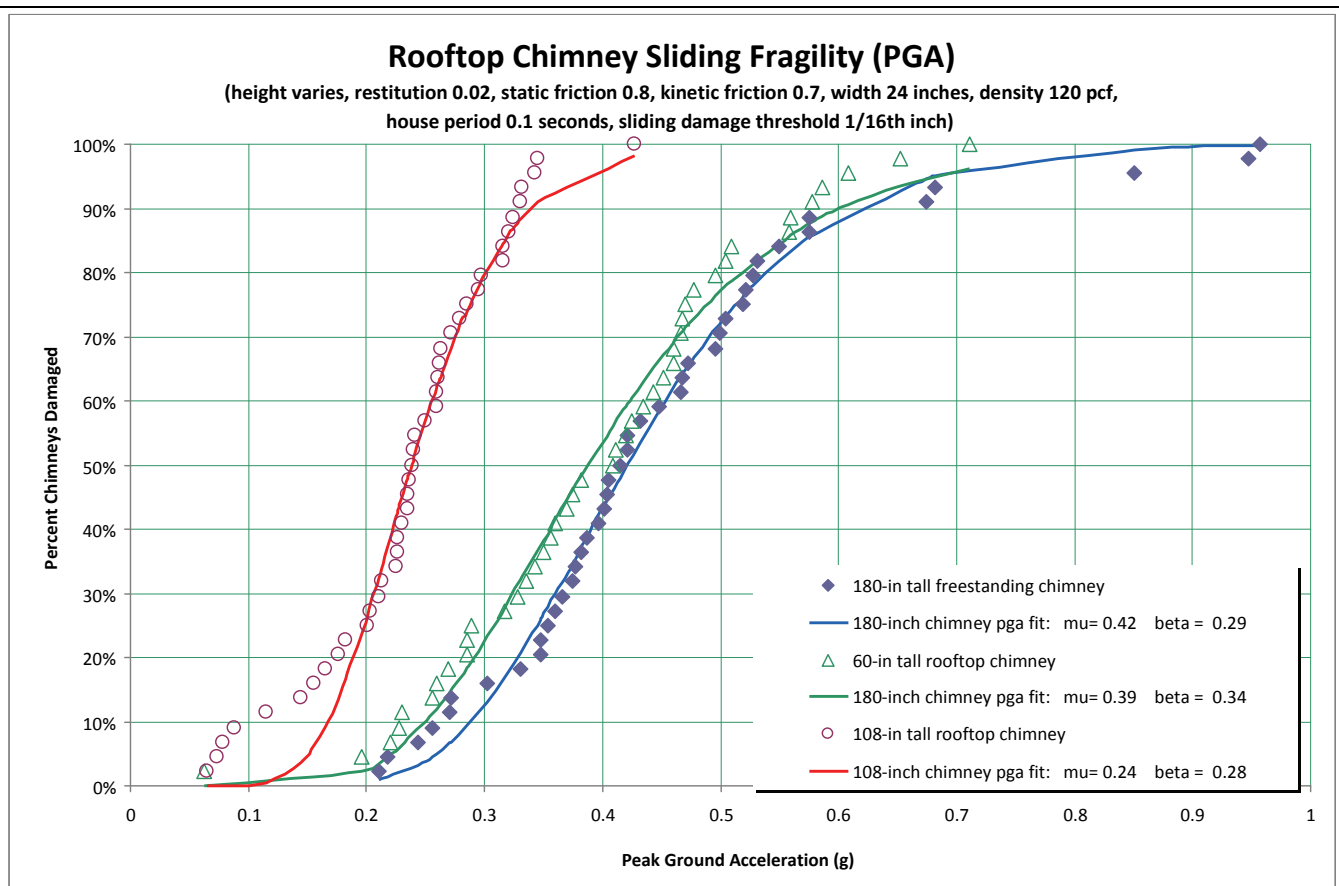


Figure 16. Sliding fragilities for rooftop chimneys of different heights.

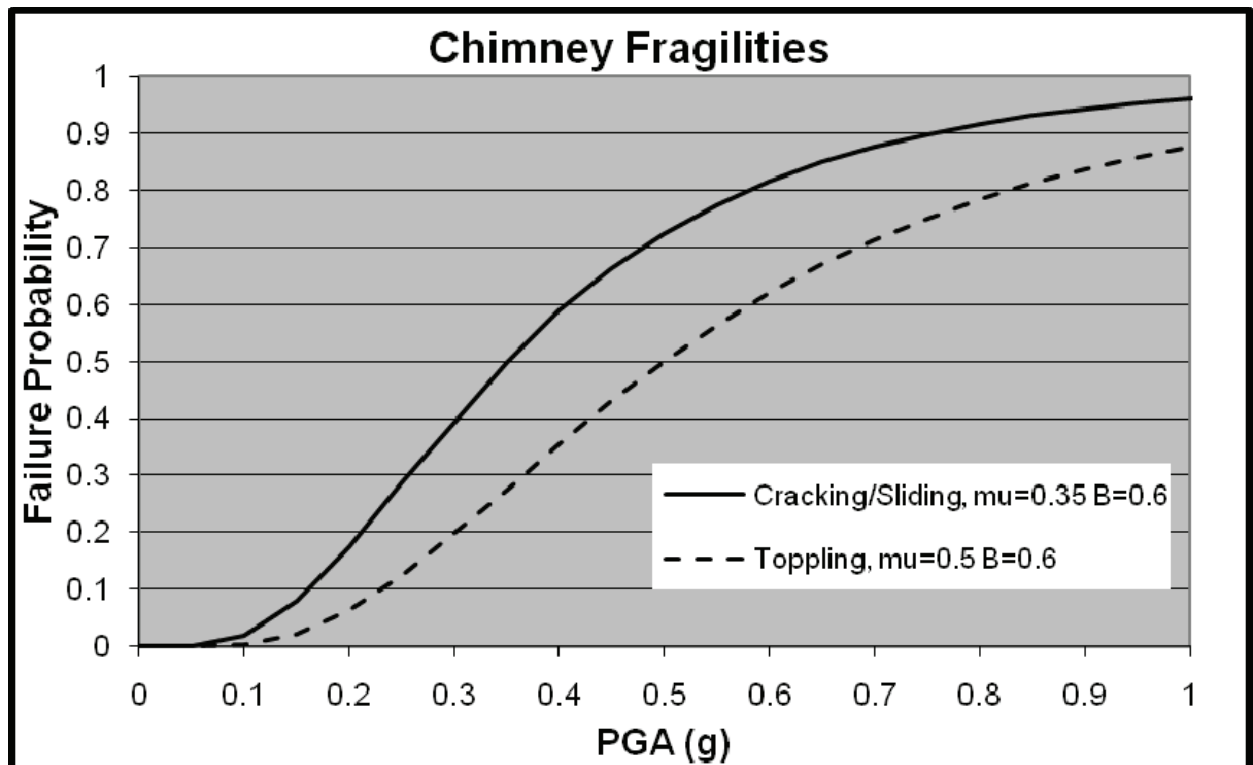


Figure 17. Proposed fragility functions for unreinforced masonry chimneys.

Consequence Analysis

Earthquake induced chimney failures pose a life safety hazard only as a result of toppling or collapse. Unfortunately, empirical data does not provide adequate data to determine the relative frequency of toppling or collapse of all or a portion of a chimney. Analytical studies suggest that relatively consistent fragility information can be obtained for toppling as well as for sliding – but within the constraints made by representing widely varying boundary conditions with simple models of either free-standing or fully-attached rigid blocks.

Chimney repair cost data is available from two sources: the LADB&S Northridge EQ repair permit dataset and the CEA dataset for insured properties damaged during the San Simeon EQ.

Repair costs for chimneys damaged in the San Simeon EQ presented in Figure 18 as a function of PGA show no trend with shaking intensity. The data are however grouped into two subsets: repair cost estimated at \$2000 or less and repair cost estimated at more than \$5000. This split suggests that the lower cost estimates reflect chimney repair while the higher values reflect chimney replacement. For the 27 damaged chimneys, the dollar cost of chimney repair can be represented by a mean value of \$6,089 with a dispersion of \$4,717 (2002 Dollars).

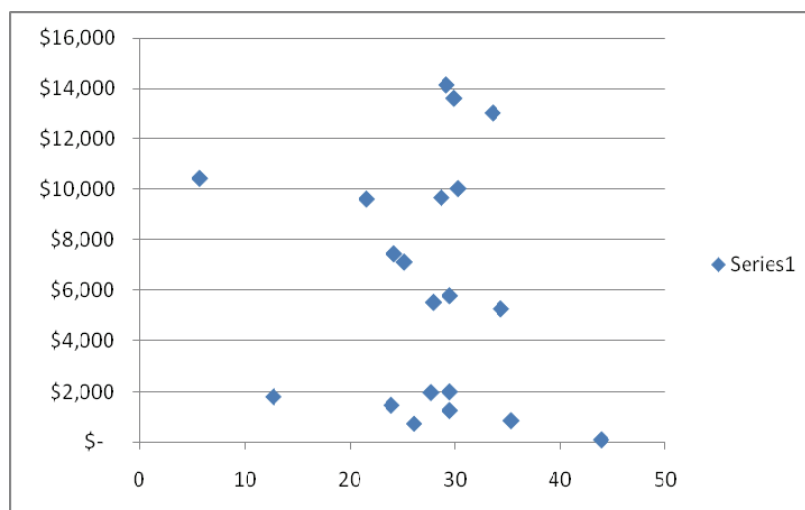


Figure 18. Cost of chimney repair following San Simeon EQ as a functions of PGA, based on earthquake insurance claims underwritten by the CEA.

Using the address field in the repair LADB&S Northridge Earthquake permit records, chimney repair valuations could be compared to site-specific PGA. Chimney repair locations, color coded by repair cost as indicated on the permit, are presented in Figure 19. (It is noted that because of plotting limitations not all of the 29,536 repairs are visible; lower valuations are generally plotted first and subsequently obscured by dots associated with higher valuation.) While overall the number and cost of chimney repair generally decreases with distance from the rupture zone, Figure 19 demonstrates that chimney repairs are often clustered in areas more likely correlated by housing density, construction vintage / quality, rather than ground motion intensity measure.

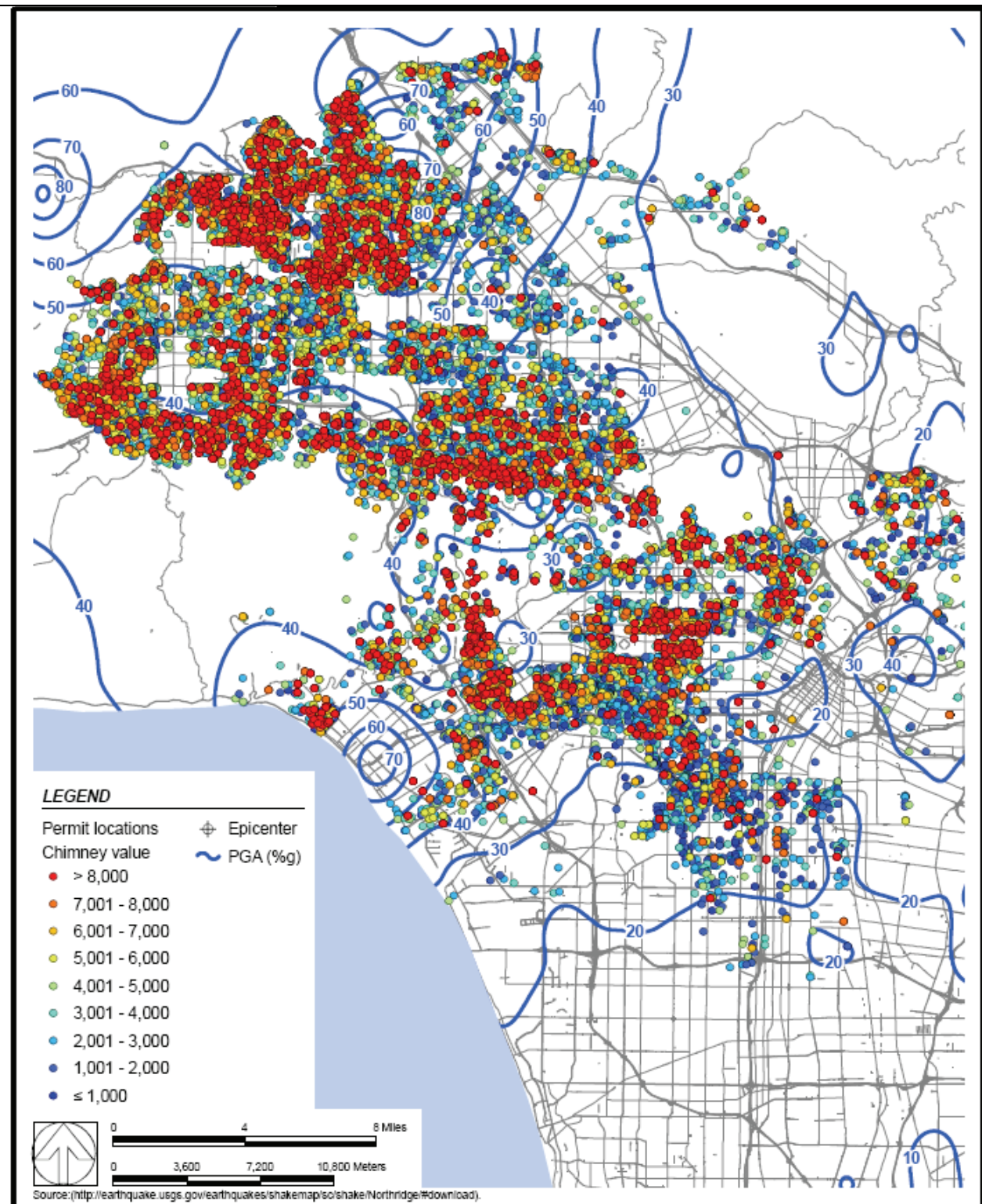


Figure 19. LADB&S permit values of chimney repair cost following the Northridge EQ plotted on ShakeMap PGA contours, based on earthquake insurance claims underwritten by the CEA.

As may be seen in Figure 20, which presents chimney repair cost as a function of site-specific PGA, there appears to be virtually no correlation between PGA and cost of chimney repair. Thus, the dollar cost of chimney repair can be represented as a mean value of \$3,350 with a dispersion of 0.5 (1994 dollars) regardless of degree of damage.

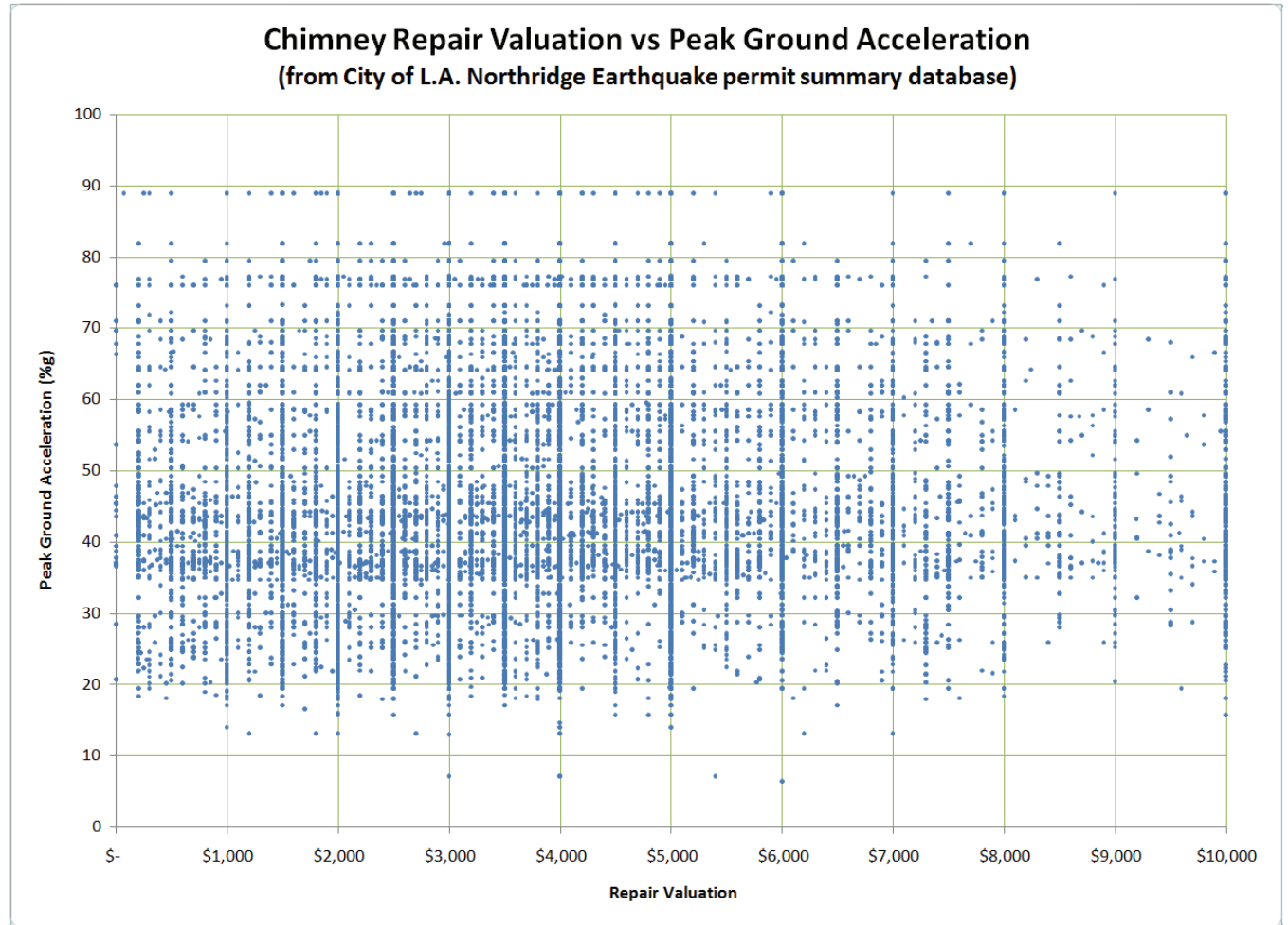


Figure 20. Permit value of chimney repair cost in the City of Los Angeles following the Northridge EQ, as a function of PGA.

It must be noted that chimney repair in the City of Los Angeles was based on prescriptive criteria set forth in *LADB&S (2001)* (the most recent version of a document first issued in 1994). Adoption of similar criteria in a community will likely result in cost of repair similar to that experienced in Los Angeles following the Northridge EQ. Communities with lax repair requirements will likely see lower repair costs. In practice, many chimneys with minor cracking or small offsets will simply be patched or tuck pointed.

REFERENCES CITED

Aslam M, WG Godden, and DT Scalise (1980) Earthquake Rocking Response of Rigid Bodies, *Journal of the Structural Division – Proceedings of the American Society of Civil Engineers*, Vol. 106, No. ST2, February 1980.

ATC-38 (2001) Database on the performance of structures near strong-motion recordings: 1994 Northridge California Earthquake, Applied Technology Council, 2001.

Baker and Zareian (2009) Maximum Likelihood routine for fitting log-normal curves, personal communication with H Krawinkler.

Booth DB, RE Wells, and RW Givler, (2004) Chimney Damage in the Greater Seattle Area from the Nisqually Earthquake of 28 February 2001, BSSA v94 n3, June 2004

CEA (2009) San Simeon Earthquake chimney assessment data, personal communication between Dan Dyce and JD Osteraas.

CUREE (2010) EDA-02 General Guidelines for the Assessment and Repair of Earthquake Damage in Residential Woodframe Buildings, Consortium of Universities for Research in Earthquake Engineering, 2010.

Design Simulation Technologies, Inc (2005) Working Model 2-D 2005 <http://workingmodel.design-simulation.com/WM2D/index.php>

FEMA (2009). "Quantification of Building Seismic Performance Factors," FEMA P-695 Report, prepared by the Applied Technology Council for the Federal Emergency Management Agency, Washington, D.C

Graf WP (2009) 1994 Northridge Earthquake chimney damage data, personal communication with JD Osteraas.

Housner GW (1963) The Behavior of Inverted Pendulum Structures During Earthquakes, Bulletin of the Seismological Society of America, Vol. 53, No. 2, February 1963.

Ishiyama, Y (1982) Motions of Rigid Bodies and Criteria for Overturning by Earthquake Excitations, Earthquake Engineering and Structural Dynamics, Vol. 10, 635-650, 1982.

Ishiyama, Y (1984) Criteria for Overturning of Rigid Bodies by Sinusoidal and Earthquake Excitations, Proceedings of the Eighth World Conference on Earthquake Engineering, Vol. IV – Response of Structures, July 21-28, 1984.

King SA, AS Kiremidjian, P Sarabandi, and D Pachakis (2005) Correlation of Observed Building Performance with Measured Ground Motion, Stanford University, Blume Center Report No. 148, February 2005.

LADB&S (1994) Northridge Earthquake Repair Permit Database, Los Angeles Department of Building and Safety, 1994.

LADB&S (2001) Reconstruction and Replacement of Earthquake Damaged Masonry Chimneys, rev 8.17.2001, Los Angeles Department of Building and Safety, August 2001.

Lopez-Garcia, D and TT Soong (2003) Sliding Fragility of block-type non-structural components. Part 1: Unrestrained components, Earthquake Engng. Struct. Dyn. 2003; 32:111-129

Makris, N, D Konstantinidis (2003) The rocking spectrum and the limitations of practical design methodologies, Earthquake Engng. Struct. Dyn. 2003; 32:265-289.

McMullin KM, T Garvey, S Parrott (2001) The February 28, 2001 Nisqually Earthquake: Reconnaissance Report, Collaborative for Disaster Mitigation, Report CDM/2001/01, San Jose State University Foundation, April 25, 2001.

Meisl CS, Elwood KJ, and Ventura CE (2007) Shake Table Tests on the Out-of-Plane Response of Unreinforced Masonry Walls, Canadian Journal of Civil Engineering, Vol. 34, 2007.

NAHB Research Center (2003) "New Madrid seismic zone: overview of earthquake hazard and magnitude assessment based on fragility of historic structures," US Department of Housing and Urban Development, Office of Policy Development and Research, <http://www.huduser.org/publications/pdf/newmadrid.pdf>, May 2003

Pena, F, et al, (2007) On the dynamics of rocking motion of single rigid-block structures - Dynamics of rocking block, Earthquake Engng. Struct. Dyn. 2007; 36:2383-2399.

Purvance, MD, et al (2008) Free standing block overturning fragilities: Numerical simulation and experimental validation, Earthquake Engineering and Structural Dynamics, 2008: 37:791-808

Scholl RE (1974) Statistical Analysis of Low-rise Building Damage Caused by the San Fernando Earthquake, BSSA v64 n1, 1974

Sharif I, Meisl CS, and Elwood KJ (2007) Assessment of ASCE 41 Height-to-Thickness Ratio Limits for URM Walls, Earthquake Spectra, Vol. 23, No. 4, November 2007.

Spanos PD, and Koh AS (1969) Rocking of Rigid Blocks Due to Harmonic Shaking, Journal of Engineering Mechanics, Vol. 110, No. 11, November 1984.

Steinbrugge, Cloud, and Scott (1970) The Santa Rosa Earthquakes of October 1, 1969, U.S. Department of Commerce.

Steinbrugge, Schader, Bigglestone and Weers (1971) San Fernando Earthquake, February 9, 1971, Pacific Fire Rating Bureau

Taniguchi, T (2002) Non-linear response analysis of rectangular rigid bodies subjected to horizontal and vertical ground motion, Earthquake Engng Struct. Dyn 2002; 31:1481-1500.

USGS The Shakeout Scenario for Wood Frame Buildings
<http://www.colorado.edu/hazards/shakeout/woodframe.pdf>

Whitman RV (2002). "Ground motions during the 1755 Cape Ann earthquake," Proceedings of the Seventh U.S. National Conference on Earthquake Engineering, July 21-25, Boston, MA.

Yim CS, Chopra AK, and Penzien J (1980) Rocking Response of Rigid Blocks to Earthquakes, Earthquake Engineering and Structural Dynamics, Vol. 8, 1980.

Zhang, J, Makris, N (2001) Rocking Response of Free-Standing Blocks Under Cycloidal Pulses, University of California Postprints, Paper 2628, 2001.

Revision history

1.0	30 Nov 2010	Initial release
2.0	08 Dec 2010	Revisions to all sections Issued to REB